DESIGN AND IMPLEMENTATION OF INTEGRATED BOOST RESONANT FULL BRIDGE DC-DC CONVERTER FOR PHOTOVOLTAIC APPLICATIONS

K.CHANDRIKA, S.DHAMRAI SELVI, S.SIVAGANESHAN

ABSTRACT

Design and implementation of an integrated boost full bridge resonant converter with low circulating energy, galvanic isolation, simple control, as well as simple gate drive and control and high efficiency across a wide input and load range. Photovoltaic effect is used for power conditioning required maximum power point tracking to counteract the effects of panel mismatch, shading and general variance in power output during a daily cycle. The solar dc outputs is boosted using dc-dc converter and the dc boosted voltage is converted ac voltage source using micro inverter.

Index Terms—Integrated boost resonant (IBR), isolated dc–dc microconverter, photovoltaic (PV).

I. INTRODUCTION

POWER conversion for photovoltaic (PV) applications, as opposed to more conventional dc–dc converter configurations, requires an adaptable system that is capable of responding to a wide range of input voltage and current conditions. As pre- viously stated in the literature, PV voltage varies significantly with panel construction and operating temperature, while the PV current changes largely due to solar irradiance and shading conditions [2]. If a converter is designed only for high peak efficiency, oftentimes the range of conditions common to many PV installations will force the converter into another operating region where it is much less efficient.

Also of interest in the PV PCS design process is the necessity of galvanic isolation between the PV panel and the electric utility system. While an ungrounded, grid-connected PV array is permitted by many electric codes, galvanic isolation can be preferred for various reasons. Most notable among these are improved voltage boost ratio, reduced ground leakage current ,and overall safety improvement during fault conditions .
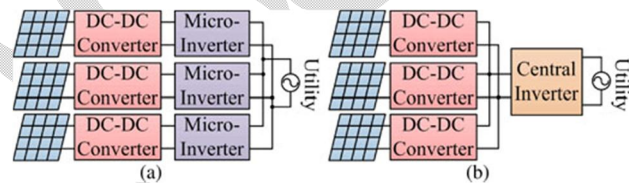

Fig. 1Distributed (a) microinverter and (b) microconverter system

As several authors have already proposed, distributed maximum power point tracking (MPPT) can achieve much better energy harvesting over systems that are completely centralized [2]. Researchers have also concluded that a system structure with the PV panels connected in parallel can be much more productive in low-light and partially shaded conditions than a series-connected system [3]–[7]. These concerns arguably make the single-panel PV micro inverter (dc–ac), or at least an isolated micro converter (dc–dc), an attractive option from a strictly performance-based analysis. In either system, the dc–dc stage implements local MPPT optimization, while the second stage attempts to regulate the dc-link voltage by sending power to the utility grid. Block diagrams showing the microinverter and microconverter system structures are provided in Fig. 1. It is this combination of high CEC efficiency, galvanic isolation, and a localized, distributed approach

to energy conversion that has prompted the proceeding technical development. One popular option for the dc–dc conversion stage is a simple continuous conduction-mode (CCM) flyback converter [18], [19]. It has the benefit of simple construction and low circulating energy. However, the switching loss for both the primary switch and the diode can be quite large, and the overall system efficiency is typically low (<90%). Improvements in flyback efficiency can be made using variants such as zero-voltage transition or active clamp, both of which use the transformer leakage inductance as a resonant element to achieve zero-voltage switching (ZVS) across the main device [10], [11]. However, this effectively trades switching loss for circulating energy, reducing efficiency at high line or low power. Another more complex effort involves transitioning between different circuit topologies at different load/line conditions thereby increasing control and system complexity [12].Another option is the series-resonant converter, and more recently the LLC resonant converter, both of which operate on a similar principle and, typically, use a variable frequency control to adjust the output voltage [13]–[15]. When the series-resonant, or LLC converter, is operated near the resonant frequency of the tank circuit, the converter achieves nearly ZVS and zero-current switching (ZCS) with very low circulating energy, giving it a high peak efficiency. However, as the operating frequency diverges from the resonant frequency, the amount of circulating energy increases. Unfortunately, the normal conditions for PV conversion will often push the converter significantly away from the optimum switching frequency, causing the CEC efficiency to suffer. Several authors have proposed methods to extend the line and load range of the LLC, once again complicating the circuit topology and control [16]–[18]. This approach has the benefit of almost no switching loss, little or no circulating energy, very high peak efficiency, and integrated isolation. However, the inverter stage must be able to regulate over a wide input range because the PV voltage fluctuates so dramatically, causing extremely poor overall system efficiency.

This concept of using the series-resonant DCX is not without merit, but the system requires an additional element to pro- vide regulation capability. The method proposed in this paper integrates a traditional boost converter element into the DCX with only the addition of a single inductor. The overall design is straightforward and may be controlled using simple fixed- frequency PWM with only the need to observe limitations on the maximum and minimum duty cycle. For PV applications, this circuit satisfies the need for galvanic isolation, low switching loss (the output diodes achieve ZCS), minimal circulating energy, as well as simple gate drive and control. In the following sections, the authors will discuss the synthesis of the topology, key waveforms and operational characteristics, design procedure and loss analysis, as well as experimental results for a 250-W prototype.

II. CONVERTER SYNTHESIS AND OPERATION

When considering the series-resonant DCX as part of this new hybrid circuit, it is important to notice the half-wave resonant behavior by which it operates. During the on-period of either switch a resonant circuit is formed by a combination of the input-side capacitors, the output-side capacitors, and the transformer leakage inductance. The unidirectional nature of the output diodes prevents this circuit from resonating perpetually, and instead, only a resonant period consisting of one half-sine wave is visible. Provided that this resonant period is allowed to complete fully before the primary-side switches change states, the series-resonant circuit is naturally soft-switching on both turn-on and turn-off (ZVS and ZCS). If both resonant periods are allowed to fully complete, the system has no method by which to regulate the output, and the output is simply a reflection of the input. Hence, the necessary addition of another "regulating element," in this case a boost converter, is shown in Fig. 2. The boost converter regulates the effective input voltage to the series-resonant converter, allowing it to run as a DCX with high efficiency. The cost is two additional transistors, with their associated gate drive requirements, and some additional switching and conduction loss.
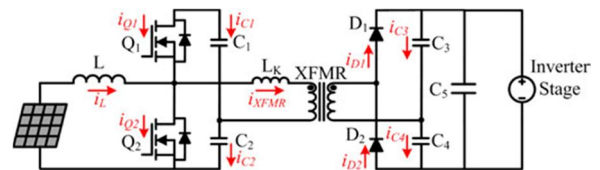

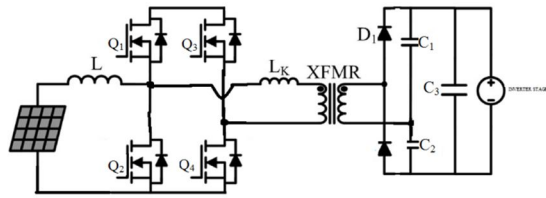Fig. 2. Resonant half-bridge with boost converter

Fig 2. Full Bridge converter

This circuit may be further simplified by integrating the sys- tem so that the boost converter function is implemented by the original four MOSFETs. A straightforward method to under- stand this is to directly tie the input inductor to the midpoints of both active switching legs simultaneously. Note that this change directly ties the inductor to one terminal of the transformer. This additional connection renders the upper MOSFETs and as well as the lower MOSFETs in parallel, so long as their switching patterns are synchronized. Thus, the circuit may be simplified, with the additional connection and the removal of QX and QY ,into the topology shown in Fig. 3. Because the now upper and lower FETs (Q1,Q2, Q3 and Q4) are effectively replacing two parallel FETs, they carry the combined current from the original four switches. Also, as long as the resonant behavior is allowed to complete, the output diodes, D1 and D2 , still achieve ZCS.
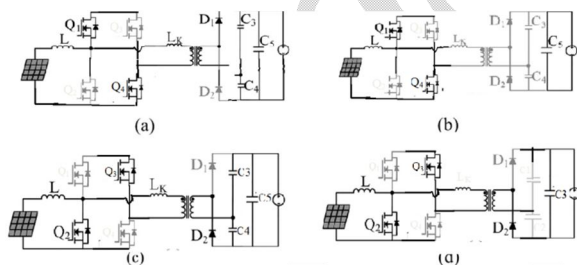

Fig 4: full bridge converter operation.

In the BFB, the operating currents are that of the hard-switching half-bridge, giving the converter a poor power factor at the transformer. This makes it difficult for the converter to achieve a wide range of operation, even with ZVS. Also, the voltage transfer ratio is highly nonlinear, leading to much more complex control requirements.

On the other hand, this new circuit features a very simple voltage transfer ratio, given in (1), where n is the transformer turns ratio, and D is the duty cycle of the lower switch, Q2 .Unlike the BFB, this transfer ratio is constant over both input load and frequency.

$$\frac{V_{out}}{V_{in}} = \frac{n}{1-D}. \tag{1}$$

Mode 1 [t0 < t < t1]: Beginning with the turn- off of Q2 and Q3 prior to t0 , the current in the input inductor L flows into the body diode of Q1 and Q4 , discharging its parasitic capacitance. This allows Q1 and Q4 to be turned ON under ZVS conditions at t0 . At this time, the upper input-side capacitor C1 begins resonating with the transformer leakage inductance Lk and the output-side capacitors, C3 and C4 , through D1 .. Once the transformer current resonates back to zero, D1 prevents the continued resonating in the reverse direction depending mode 1.

Mode 2 [t1 < t < t2]: Q1 and Q4 is still active, yet it is only conducting the input inductor current, which is still decreasing, a pathway which is shown in Fig. 4(b). The resonant elements all conduct zero current during this interval. Only C5 continues discharging into the load at this time. Mode 2 ends with the turn-off of Q1 and Q4 and the subsequent turn on of Q2 and Q3.

Mode 3: [t2< t < t3]: After the turn-off Q1 and Q4 , but prior the turn-on of Q2 , the inductor current is still shunted into charging this time through the body diode of Q1 , and still decreasing almost linearly. When Q2 and Q3 is turned ON, the body diode of Q1 and Q4 is hard- commutated, causing some switching loss. At t2 , C2 begins to resonate with Lk and the parallel combination of C3 and C4 , through the diode D2 . Simultaneously, the inductor current also flows through Q2 and Q3 , increasing linearly. During this interval, Q2 and Q3 carries the sum of the transformer current and the inductor current. Thus, the rms current through Q2 is significantly larger than that of Q1 , which carries the difference of the two currents. Once the transformer current resonates back to zero, D2 blocks the continued oscillation, marking the end of mode 3.

Mode 4 [t3 < t < t4]: The inductor current continues to flow through the lower device, increasing until Q2 and Q3 is turned OFF and the circuit returns to mode 1. Also, during both modes 3 and 4. Q1 effectively isolates the upper capacitor from charging or discharging.

Note that there is a significant difference in the

circuit behavior between the two resonant modes (1 and 3). During mode 3, C1 is effectively isolated from the rest of the circuit due to the presence of Q1 . However, during mode 1, C2 has an ac discharge path through the PV source and the input inductor,allowing the two input capacitors (C1 and C2) to appear in parallel, though the resonant current is not shared evenly between them. Thus, the length of mode 1 can be significantly longer than mode 3, depending on the relative sizing of C1 –C3 and the transformer turns ratio n.

III.DESIGN PROCEDURE AND LOSS ANALYSIS

A. Determining Duty Cycle Limits From Input Requirements

The most critical element of this design procedure is the identification of the input voltage requirements, so that the duty cycle range is fully utilized. With this converter, there is a direct tradeoff between increased input range and lower rms currents in the circuit. The most basic method involves setting the maximum and minimum duty ratios such that the middle of the input range results in a 50% duty cycle at the converter.

B.DETERMINING MAXIMUM RESONANT PERIOD LENGHTS

With the maximum and minimum duty ratios known, the limits for the resonant periods Tres1 and Tres2 may be calculated based on the desired switching period Tsw.

### C. Design Input Inductor Based on Allowable Current Ripple

Multiple criteria may be used for designing the input inductor. In PV applications, especially for accurate MPPT, the inductor current ripple must be regulated. The following equation specifies the input inductance based on the maximum allowable current ripple.

D. Resonant Capacitor Design

With the magnetics design complete, it is now possible to design the resonant capacitors C1 –C2 . In order to reduce the rms currents in the circuit, the resonant period needs to be as close to the calculated maximum as possible. Because the leakage inductance of the transformer, Lk , is involved in the resonant

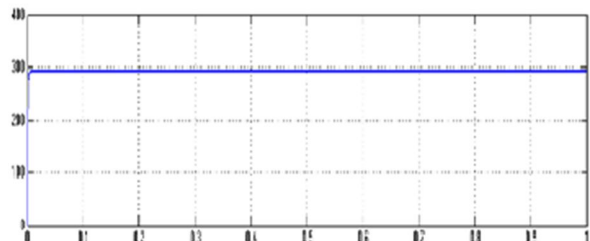circuit and is a consequence of the transformer design in step 3, it is left as a constant here
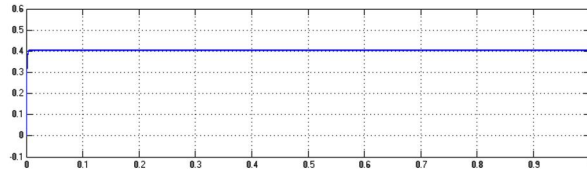
SIMULATION RESULTS:
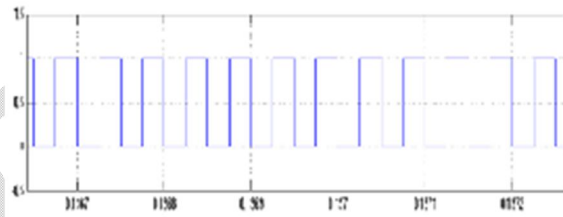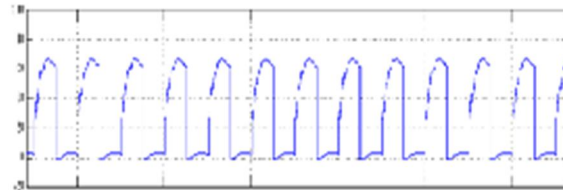
DRAIN TO SOURCE VOLTAGE
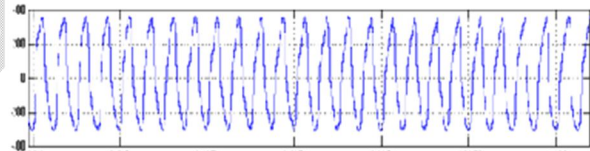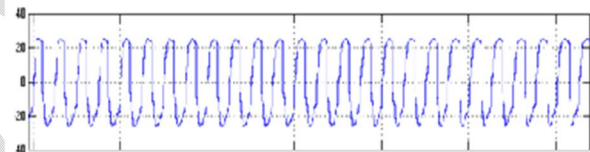
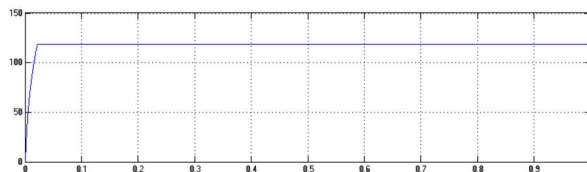**TRANSFORMER PRIMARY TO SECONDARY VOLTAGE**

OUTPUT VOLTAGE

OUTPUT CURRENT

OUTPUT POWER

V. CONCLUSION

As a solution for providing efficient, distributed PV con- version, an isolated boost resonant converter has been pro- posed. The system is a hybrid between a traditional CCM boost converter and a series-resonant full-bridge, employing only four active switches. The synthesis of the converter was described along with the circuit operating modes and key waveforms. The design process was then defined, with a focus on the unique process, requiring only consideration of the resonant period length in selecting a valid converter duty cycle range. Also pro- vided was a detailed theoretical loss analysis, along with formulas for calculating the rms values of important waveforms.

The principle advantages of utilizing this topology were as follows:
Switching losses are reduced.
Reduced Filter size
Reduced transformer size

REFERENCES

1.Design and implementation of Integrated Boost Resonant Full bridge DC-DC Converter for Photovoltaic Applications.IEEE transaction on power electronics.,vol.28, no.3 ,March 2013

2.] A. S. Masoum, F. Padovan, and M. A. S. Masoum, "Impact of partial shading on voltage- and current-based maximum power point tracking of solar modules," in Proc. IEEE PES General Meet., 2010, pp. 1–5.

3. Q. Li and P. Wolfs, "Recent development in the topologies for photovoltaic module integrated converters," in Proc. IEEE Power Electron. Spec. Conf.,2006, pp. 1–8

4. L. Gao, R. A. Dougal, S. Liu, and A. P. Iotova, "Parallel-connected solar PV system to address partial and rapidly fluctuating shadow conditions," IEEE Trans. Ind. Electron., vol. 56, no. 5, pp. 1548–1556, May 2009.

5. R. Gules, J. De Pellegrin Pacheco, H. L. Hey, and J. Imhoff, "A maximum power point tracking system with parallel connection for PV stand-alone applications," IEEE Trans. Ind. Electron., vol. 55, no. 7, pp. 2674–2683, Jul. 2008.

6. B. Liu, S. Duan, and T. Cai, "Photovoltaic dc-building-module-based BIPV system: Concept and design considerations," IEEE Trans. Power Electron., vol. 26, no. 5, pp. 1418–1429, May 2011.

7. W. Xiao, N. Ozog, and W. G. Dunford, "Topology study of photovoltaic interface for maximum power point tracking," IEEE Trans. Ind. Electron., vol. 54, no. 3, pp. 1696–1704, Jun. 2007.

8. L. Zhang, K. Sun, Y. Xing, L. Feng, and H. Ge, "A modular grid-connected photovoltaic generation system based on dc bus," IEEE Trans. PowerElectron., vol. 26, no. 2, pp. 523–531, Feb. 2011

9. D. C. Martins and R. Demonti, "Photovoltaic energy processing for utility connected system," in Proc. Ind. Electron. Soc., 2001, vol. 2, pp. 1292–1296.

10. E. Roman, R. Alonso, P. Ibanez, S. Elorduizapatarietxe, and D. Goitia, "Intelligent PV module for grid-connected PV systems," IEEE Trans. Ind. Electron., vol. 53, no. 4, pp. 1066–1073, Jun. 2006.

11. Y.-C. Hsieh, M.-R. Chen, and H.-L. Cheng, "An interleaved flyback con- verter featured with zero-voltage transition," IEEE Trans. Power Elec-tron., vol. 26, no. 1, pp. 79–84, Jan. 2011.

12. G. Spiazzi, P. Mattavelli, and A. Costabeber, "High step-up ratio flyback converter with active clamp and voltage multiplier," IEEE Trans. Power Electron., vol. 26, no. 11, pp. 3205–3214, Nov. 2011.

13. M. Fornage, "Method and apparatus for converting direct current to alter- nating current," U.S. Patent 7 796 412, Sep. 14, 2010.

14.Y. Gu, L. Hang, Z. Lu, Z. Qian, and D. Xu, "Voltage doubler application in isolated resonant converters," in Proc. Ind. Electron. Soc., 2005, p. 5.

15.B. Lu, W. Liu, Y. Liang, F. C. Lee, and J. D. van Wyk, "Optimal design methodology for LLC resonant converter," in Proc. Appl. Power Electron. Conf., 2006, p. 6.

16. J. F. Lazar and R. Martinelli, "Steady-state analysis of the LLC series

resonant converter," in Proc. Appl. Power Electron. Conf., 2001, vol. 2, pp. 728–735.

17. Z. Liang, R. Guo, J. Li, and A. Q. Huang, "A high-efficiency PV module- integrated dc/dc converter for PV energy harvest in FREEDM systems,"

IEEE Trans. Power Electron., vol. 26, no. 3, pp. 897–909, Mar. 2011. [27] B.-G. Chung, K.-H. Yoon, S. Phum, E.-S. Kim, and J.-S. Won, "A novel

LLC resonant converter for wide input voltage and load range," in Proc.

Int. Conf. Power Electron./ECCE Asia, 2011, pp. 2825–2830.

18. H. Hu, X. Fang, Q. Zhang, Z. J. Shen, and I. Batarseh, "Optimal design considerations for a modified LLC converter with wide input voltage range capability suitable for PV applications," in Proc. Energy Convers. Congr. Expo., 2011, pp. 3096–3103.

\